JACS
JOURNAL OF THE AMERICAN CHEMICAL SOCIETY
Communication
pubs.acs.org/JACS

Chemical Dynamics of the First Proton-Coupled Electron Transfer of Water Oxidation on TiO_2 Anatase

Jia Chen,* Ye-Fei Li,* Patrick Sit, and Annabella Selloni

Department of Chemistry, Princeton University, Princeton, New Jersey 08544, United States

Supporting Information

ABSTRACT: Titanium dioxide (TiO_2) is a prototype, water-splitting (photo)catalyst, but its performance is limited by the large overpotential for the oxygen evolution reaction (OER). We report here a first-principles density functional theory study of the chemical dynamics of the first proton-coupled electron transfer (PCET), which is considered responsible for the large OER overpotential on TiO_2. We use a periodic model of the TiO_2/water interface that includes a slab of anatase TiO_2 and explicit water molecules, sample the solvent configurations by first principles molecular dynamics, and determine the energy profiles of the two electronic states involved in the electron transfer (ET) by hybrid functional calculations. Our results suggest that the first PCET is sequential, with the ET following the proton transfer. The ET occurs via an inner sphere process, which is facilitated by a state in which one electronic hole is shared by the two oxygen ions involved in the transfer.

The photocatalytic splitting of water on semiconductor electrodes has fascinated and intrigued researchers for over 40 years.[1−4] Overall, the water splitting process consists of two half-reactions, the oxygen evolution reaction (OER) at the (photo)anode, and the hydrogen evolution reaction (HER) at the cathode of a (photo)electrochemical cell. Of the two, the OER is the major obstacle as it generally requires a large overpotential which causes substantial energy losses.[5] This difficulty is present also for TiO_2, one of the most important (photo)anode materials for the OER due to its abundance and high stability in both acidic and alkaline conditions.[6−11] Intense research efforts have been devoted to reducing the OER overpotential on TiO_2, for instance by doping with various elements.[8,12,13] However, it is still unclear how to design a photocatalyst with high OER activity, largely because the kinetics of the OER is not well-known. An atomic-level understanding of the OER kinetics on TiO_2 not only would be of great scientific interest, but could also be helpful for the design of (photo)electrochemical water splitting cells with improved efficiencies.

The mechanism of O_2 evolution on TiO_2 surfaces has been extensively investigated.[7,9−11] Wilson first identified the formation of oxidative species on a TiO_2 anode by electrochemical scanning.[14] Using the same technique, Salvador et al. suggested that Wilson's surface species may be attributed to adsorbed H_2O_2, produced by the coupling of surface OH radicals.[15] By using in situ infrared (IR) adsorbed spectroscopy, Nakamura et al. proposed the occurrence of surface OO and OOH species,[16,17] later confirmed by DFT calculations.[18] DFT calculations of the OER energetics also showed that the first proton coupled electron transfer (PCET) is the rate determining step on both rutile[19] and anatase[18] TiO_2 (the most stable and most photocatalytically active TiO_2 phases, respectively.) Altogether, it is generally agreed that the oxidation of water is initiated by the formation of surface-trapped photoholes. These holes (h^+) can oxidize water to O_2 through four sequential proton coupled electron transfer (PCET) steps. For example, the following steps are frequently assumed:[19] (i) $^*H_2O + h^+ \rightarrow {}^*OH + H^+$; (ii) $^*OH + h^+ \rightarrow {}^*O + H^+$; (iii) $^*O + H_2O(l) + h^+ \rightarrow {}^*OOH + H^+$; (iv) $^*OOH + h^+ \rightarrow O_2 + H^+$ (* denotes a TiO_2 surface site, *X is an adsorbed X species, $H_2O(l)$ a liquid water molecule, and H^+ a solvated proton).

There is significant evidence that kinetic effects are also essential for the OER. Transient absorption spectroscopy (TAS) measurements of trapped photoholes in nanocrystalline (nc) TiO_2 have been reported by several groups.[20−23] The decay of the photoholes can be described by two exponentials. The fast component (with a decay time of the order of 1 μs or less) is attributed to electron−hole recombination, the other to the reaction with surface-adsorbed species.[23] On nc-TiO_2 photoanodes the required photohole lifetime for O_2 evolution is estimated to be ∼30 ms at pH 12.7[22] and ∼0.2 s at pH ≈ 6.5,[21] the faster rate of water oxidation at higher pH suggesting a change in the water oxidation mechanism with pH. Similarly, photoluminescence (PL) measurements on rutile TiO_2 have shown that the PL intensity, which is proportional to the recombination rate of the photogenerated carriers, sharply decreases at pH larger than ∼4[24] (a value close to the point of zero charge, pzc ∼5, of TiO_2), indicating that the OER rate increases at higher pH. These results cannot be explained on the basis of pure energetics. In fact theoretical analysis of the OER energetics shows that the overpotential does not change with pH,[19] thus suggesting that the enhanced activity at high pH could originate from kinetic effects.

To obtain insight into the kinetics of the OER, we have carried out a theoretical study of the first PCET

$$^*H_2O + h^+ \rightarrow {}^*OH + H^+ \quad (1)$$

which is generally considered the rate-determining step of the OER, at the interface between anatase TiO_2(101) and liquid water.[18] Our results indicate that the proton and electron

Received: October 18, 2013
Published: December 5, 2013

dx.doi.org/10.1021/ja410685m | J. Am. Chem. Soc. 2013, 135, 18774−18777

transfers are not concerted but rather sequential, with the proton transfer (PT) preceding the electron transfer (ET). The PT has a significant activation energy, in the range 0.2−0.5 eV, whereas the following ET is essentially barrierless, in agreement with recent TAS experiments.[25] On the basis of these results, the higher OER activity that is observed experimentally at high pH can be also readily explained.

Investigation of the process (1) is theoretically and computationally challenging. A first requirement is to correctly describe the surface-trapped holes, which play a key role in the OER. Since hole relaxation to the top of the valence band is several orders of magnitude faster than the following surface chemical reaction,[22,23,26] it is reasonable to describe the surface-trapped hole by ground state density functional theory. However, standard local or semilocal DFT functionals are unable to capture the polaronic character of the surface hole.[27] Instead, we use a periodic hybrid functional approach, which has been found to work quite well in previous studies.[28] A further requirement is to adequately describe the environment, the water/TiO_2 interface, where the process takes place. To generate well-equilibrated configurations of the interface, we carried out DFT-based first principles molecular dynamics[29] (FPMD) simulations of 10 ps duration on a relatively large TiO_2/water model system (see Figure 1 and Supporting Information [SI]). We then selected three well-separated configurations along the FPMD trajectory (Figure S1, SI), in each case removed one electron (i.e., created a hole), and performed a geometry relaxation using the PBE0[30] hybrid functional. The limitation to only three configurations is motivated by the high computational cost of the periodic hybrid calculations for the large systems of interest in this work. The relaxed geometries were finally used to calculate the potential energy surfaces of the PCET (computational details in the SI). Specifically, for each investigated configuration we calculated the PT energy profiles in the two electronic states relevant to the electron transfer, i.e. the state with the hole localized on the oxygen (O_a) of an adsorbed water molecule (denoted *water-hole state*), and that with the hole localized on a surface 3-fold coordinated oxygen atom (O_{3c}) close to O_a (denoted *surface-hole state*). Interestingly, we found that holes often tend to be localized on terrace O_{3c} sites, which is at variance with previous studies in vacuo[28] where a hole was found to localize preferentially at bridging O_{2c} sites. This difference is due to the fact that, in aqueous surrounding, the bridge O_{2c} accepts H-bonds from the adjacent water molecules,[31] while no H-bond is present between O_{3c} and adjacent water molecules (see Figure 1; similar structures are found in all examined snapshots). The H-bonds stabilize O_{2c} and make it a less favorable trapping site for a hole; therefore, here we take the surface O_{3c} as the trapping site for the hole. We used the distance difference between O_a−H and O_b−H, $\Delta d_{O-H} = d(O_a-H) - d(O_b-H)$ (see Figure S2), as the reaction coordinate for the PT, where H is the transferring proton and O_b is the oxygen atom of a water next to the adsorbed H_2O_a molecule.

The PCET energy profiles for a selected snapshot along the FPMD trajectory are shown in Figure 2. Each point on these curves was obtained by constrained minimization using the electronic wave function from the previous step as the initial guess, which maintains the energy profile as close as possible to the diabatic potential energy surfaces. Analogous results for two additional snapshots are reported in Figure S3; while the different solvation configurations do affect quantitatively the

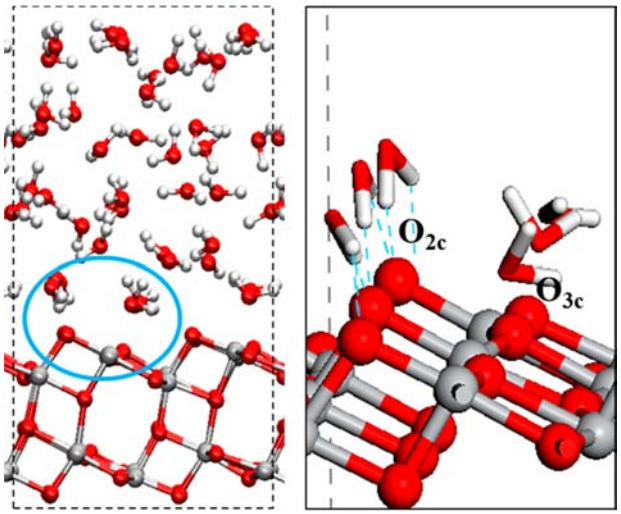

Figure 1. (Left) Side view of the system used to model the TiO_2/water interface. The model includes a periodic slab with two TiO_2 layers of 24 TiO_2 units and 48 water molecules at a density of 0.996 g/cm^3. The dashed box indicates the computational unit cell. (Right) Enlarged perspective view of the region indicated by the blue oval on the left. Some of the H-bonds between water molecules on O_{2c} surface atoms are highlighted (dashed blue lines).

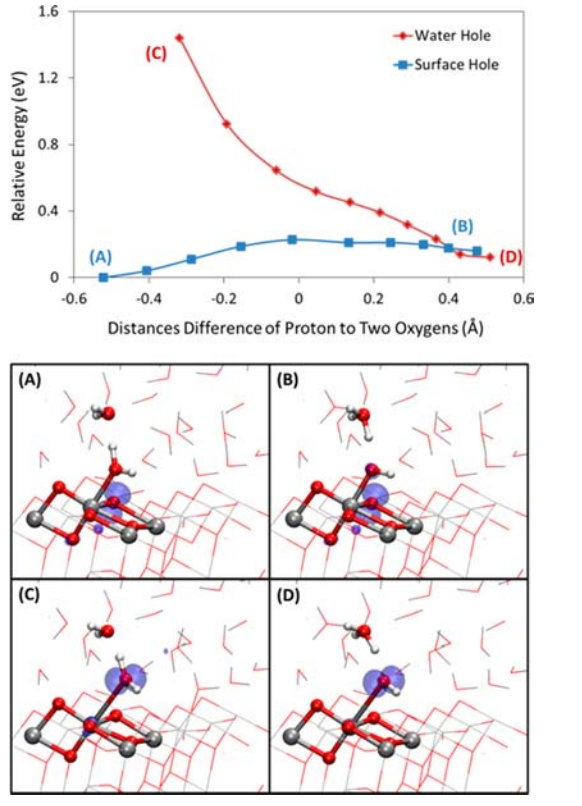

Figure 2. (Top) PT energy profiles in the surface-hole (A,B) and water-hole (C,D) states for a selected configuration along the FPMD trajectory of an anatase TiO_2(101) slab in contact with liquid water (snapshot I in Figure S1). The reaction coordinate, $\Delta d_{O-H} = d(O_a-H) - d(O_b-H)$, is defined in Figure S2. (Bottom) Spin density (0.01 au contour) of the water-hole and surface-hole states before and after the proton transfer.

dx.doi.org/10.1021/ja410685m | J. Am. Chem. Soc. 2013, 135, 18774−18777

energy profiles, the trends are the same for all three snapshots. The sequence of the proton and electron transfers in the PCET can be inferred from the intersection of the two potential energy surfaces. If the two potential energy surfaces intersect around the PT transition state (e.g., $\Delta d_{O-H} \sim 0$ Å), the PCET is concerted; if the two potential energy surfaces intersect around the PT final state (right end point of the potential energy surface), the PCET is sequential. The potential energy of the water-hole state decreases rapidly with increasing Δd_{O-H}, indicating that in this state the adsorbed water has a strong tendency to dissociate into an adsorbed OH radical and a H_3O^+. The energy profiles for the surface-hole and water-hole states become essentially degenerate around the final state of proton transfer (Figure 2), or do not intersect at all (Figure S3). This suggests that the first PCET of the OER is sequential, the ET occurring preferentially after the PT. From Figure 2 and S3 it also appears that the PT is activated, and the barrier is about 0.2, 0.4, and 0.5 eV for the three investigated snapshots.

We can understand why the process (1) tends to be sequential rather than concerted by analyzing the H-bond configurations of an adsorbed hydroxyl anion (OH^-) and a hydroxyl radical ($OH^\bullet$) at the TiO_2/water interface. As shown in Figure 3, the adsorbed OH^- accepts a short (1.58 Å) H-bond

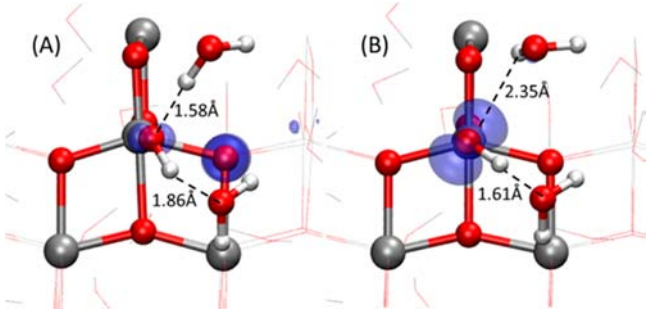

Figure 3. Top view of the spin density (0.01 au contour) and H-bond structure of (A) a hydroxide anion and a surface hole; (B) hydroxyl radical (snapshot IV in Figure S1).

and donates a long (1.86 Å) H-bond from/to nearby water. Vice versa, the $OH^\bullet$ accepts a long (2.35 Å) H-bond and donates a short (1.61 Å) H-bond from/to nearby water. In other words, an adsorbed OH^- is preferentially an H-bond acceptor, whereas a surface $OH^\bullet$ is preferentially an H-bond donor. In the final state of proton transfer, the hydroxyl that remains on the surface is forced to accept an H-bond from the nearby H_3O^+ (see B and D of Figure 2). Therefore, the configuration where the adsorbed species is an OH^- anion is energetically preferred.

Since the PCET (1) is sequential with the PT occurring before the ET, it is important to study also the kinetics of electron transfer from an adsorbed OH^- to a surface hole. Starting from the model in Figure 1, we removed a proton from an adsorbed water molecule and introduced a hole in the TiO_2 slab, so that the overall unit cell remains charge neutral. We then used the same strategy employed for the study of the PT, i.e. (i) performed a 10 ps FPMD simulation to generate well-equilibrated configurations of the solvent water molecules at the interface with the TiO_2 slab, (ii) randomly selected three snapshots in the interval 4−10 ps (see Figure S1), (iii) relaxed all the atoms in the selected snapshots using the hybrid PBE0 functional. To determine the ET energy profile, use of an appropriate reaction coordinate is essential. In this study, we found that an effective reaction coordinate is the distance (d_{O-O}) between the oxygen, O_a, of the adsorbed hydroxyl and the O_{3c} surface hole-trapping site. We then scanned the energy landscape by varying the reaction coordinate both inward, i.e from large to small d_{O-O}, and outward, i.e. from small to large d_{O-O}, as this is a useful procedure that can provide better insight into the ET process.[32] The resulting energy profiles (Figure 4) show that the electron transfer involves two steps. In

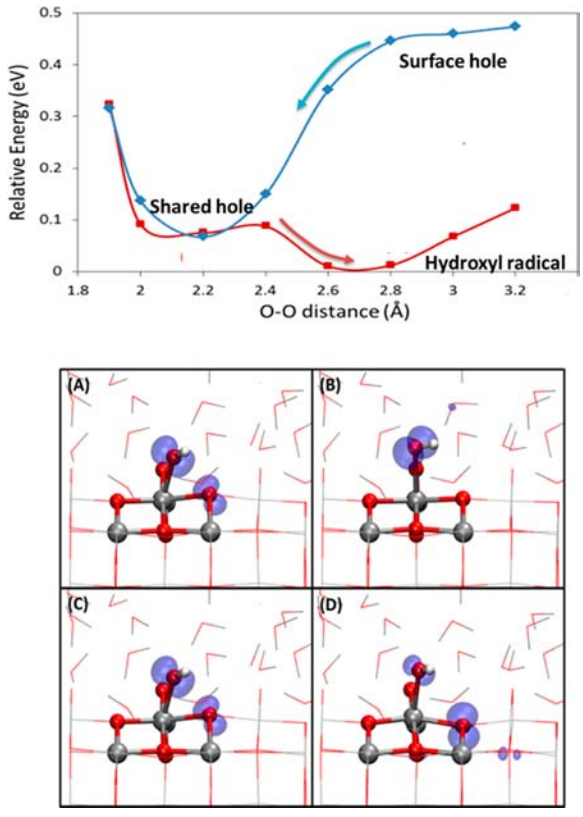

Figure 4. (Top) ET energy profiles as a function of the distance d_{O-O} between the oxygen atom of the adsorbed hydroxyl and the surface hole-trapping site (snapshot IV in Figure S1). (Bottom) Isosurfaces of the spin density (0.01 au) for the shared-hole state (A,C), hydroxyl anion + surface hole state (D) and hydroxyl radical (B). Corresponding electronic densities of states are shown in Figure S6.

the inward scan, at large d_{O-O} the hole is mainly in TiO_2 (Figure 4D) and as d_{O-O} decreases, the hydroxyl leans down toward the surface-trapped hole to form a "shared-hole" state, where the hole distributes in both O_{3c} and the hydroxyl (A and C of Figure 4). This process is barrierless. In the outward scan, i.e. as d_{O-O} increases, the hydroxyl stretches out, and the shared-hole state transforms into a more stable surface hydroxyl radical with very small (<0.1 eV) barrier. Very similar energy profiles are obtained for two other snapshots, see Figure S5, confirming that the ET has a significantly smaller barrier in comparison to the PT.

On the basis of all the above results, the kinetics of the first OER-PCET step on TiO_2 can be understood as follows. The first PCET is sequential and initiated by proton transfer. At low pH (pH < pzc), OH^- groups are scarce on the TiO_2 surface. Thus, PT is rate determining with a moderate barrier (0.2, 0.4, and 0.5 eV for the three investigated snapshots). At higher pH (pH > pzc), instead the TiO_2 surface is covered by hydroxyl anions, and the overall PCET reaction rate does not depend on

dx.doi.org/10.1021/ja410685m | J. Am. Chem. Soc. 2013, 135, 18774−18777

the PT barrier. In this case, the PCET kinetic is determined by the barrier for ET, which is significantly smaller than that of PT. As a result, the OER is faster at high pH, as indeed observed experimentally.[23,24]

Finally, our results suggest also a general strategy to enhance the overall rate of the first PCET. At low pH, the rate-determining step is the PT. To speed up the PT, we need to lower the pK_a of the reaction $*H_2O \rightarrow *OH^- + H^+$ (**2**). At high pH, the PCET is essentially barrierless, and the rate is determined by the concentration of surface OH^-. To increase the concentration of surface OH^-, we need also to lower the pK_a of (**2**). Thus, the overall OER activity could be enhanced by increasing the surface Lewis acidity, which facilitates (**2**). For instance, doping is the method most commonly utilized to modify TiO_2. Anion doping, e.g. replacing oxygen with N, C, or S, should not change the rate of the first PCET significantly, as the Lewis acid site is always a surface Ti ion, Ti_{5c}. For transition metal doping, instead, the rate of the first PCET may change significantly, due to the different Lewis acidity of transition metal dopants substituting Ti_{5c}. This is consistent with recent experiments showing significant changes of the OER overpotential on TiO_2 doped with different transition metals.[13]

■ ASSOCIATED CONTENT

Supporting Information

Computational details. PT and ET energy profiles for additional snapshots along the FPMD trajectories. This material is available free of charge via the Internet at http://pubs.acs.org.

■ AUTHOR INFORMATION

Corresponding Authors

jc4165@columbia.edu
yefeil@princeton.edu

Notes

The authors declare no competing financial interest.

■ ACKNOWLEDGMENTS

This work was supported by DoE-BES, Division of Chemical Sciences, Geosciences and Biosciences under Award DE-FG02-12ER16286. We used resources of the National Energy Research Scientific Computing Center (DoE Contract No. DE-AC02-05CH11231). We also acknowledge use of the TIGRESS high performance computer center at Princeton University.

■ REFERENCES

(1) Fujishima, A.; Honda, K. *Nature* **1972**, *238*, 37.
(2) Lewis, N. S.; Nocera, D. G. *Proc. Natl. Acad. Sci. U.S.A.* **2006**, *103*, 15729.
(3) Kudo, A.; Miseki, Y. *Chem. Soc. Rev.* **2009**, *38*, 253.
(4) Walter, M. G.; Warren, E. L.; McKone, J. R.; Boettcher, S. W.; Mi, Q.; Santori, E. A.; Lewis, N. S. *Chem. Rev.* **2010**, *110*, 6446.
(5) Dau, H.; Limberg, C.; Reier, T.; Risch, M.; Roggan, S.; Strasser, P. *ChemCatChem* **2010**, *2*, 724.
(6) Grätzel, M. *Nature* **2001**, *414*, 338.
(7) Linsebigler, A. L.; Lu, G.; Yates, J. T., Jr. *Chem. Rev.* **1995**, *95*, 735.
(8) Asahi, R.; Morikawa, T.; Ohwaki, T.; Aoki, K.; Taga, Y. *Science (Washington, DC, United States)* **2001**, *293*, 269.
(9) Fujishima, A.; Zhang, X.; Tryk, D. A. *Surf. Sci. Rep.* **2008**, *63*, 515.
(10) Diebold, U. *Surf. Sci. Rep.* **2003**, *48*, 53.
(11) Henderson, M. A. *Surf. Sci. Rep.* **2011**, *66*, 185.
(12) Chen, X.; Mao, S. S. *Chem. Rev.* **2007**, *107*, 2891.
(13) Liu, B.; Chen, H. M.; Liu, C.; Andrews, S. C.; Hahn, C.; Yang, P. *J. Am. Chem. Soc.* **2013**, *135*, 9995.
(14) Wilson, R. H. *J. Am. Chem. Soc.* **1980**, *127*, 228.
(15) Salvador, P.; Gutierrez, C. *J. Phys. Chem.* **1984**, *88*, 3696.
(16) Nakamura, R.; Nakato, Y. *J. Am. Chem. Soc.* **2004**, *126*, 1290.
(17) Nakamura, R.; Tanaka, T.; Nakato, Y. *J. Phys. Chem. B* **2004**, *108*, 10617.
(18) Li, Y.-F.; Liu, Z.-P.; Liu, L.; Gao, W. *J. Am. Chem. Soc.* **2010**, *132*, 13008.
(19) Valdés, A.; Qu, Z. W.; Kroes, G. J.; Rossmeisl, J.; Nørskov, J. K. *J. Phys. Chem. C* **2008**, *112*, 9872.
(20) Yoshihara, T.; Katoh, R.; Furube, A.; Tamaki, Y.; Murai, M.; Hara, K.; Murata, S.; Arakawa, H.; Tachiya, M. *J. Phys. Chem. B* **2004**, *108*, 3817.
(21) Tang, J.; Durrant, J. R.; Klug, D. R. *J. Am. Chem. Soc.* **2008**, *130*, 13885.
(22) Cowan, A. J.; Tang, J.; Leng, W.; Durrant, J. R.; Klug, D. R. *J. Phys. Chem. C* **2010**, *114*, 4208.
(23) Cowan, A. J.; Durrant, J. R. *Chem. Soc. Rev.* **2013**, *42*, 2281.
(24) Imanishi, A.; Okamura, T.; Ohashi, N.; Nakamura, R.; Nakato, Y. *J. Am. Chem. Soc.* **2007**, *129*, 11569.
(25) Cowan, A. J.; Barnett, C. J.; Pendlebury, S. R.; Barroso, M.; Sivula, K.; Grätzel, M.; Durrant, J. R.; Klug, D. R. *J. Am. Chem. Soc.* **2011**, *133*, 10134.
(26) Tamaki, Y.; Furube, A.; Murai, M.; Hara, K.; Katoh, R.; Tachiya, M. *Phys. Chem. Chem. Phys.* **2007**, *9*, 1453.
(27) Cohen, A. J.; Mori-Sanchez, P.; Yang, W. T. *Science* **2008**, *321*, 792.
(28) Di Valentin, C.; Selloni, A. *J. Phys. Chem. Lett.* **2011**, *2*, 2223.
(29) Car, R.; Parrinello, M. *Phys. Rev. Lett.* **1985**, *55*, 2471.
(30) Perdew, J. P.; Ernzerhof, M.; Burke, K. *J. Chem. Phys.* **1996**, *105*, 9982.
(31) Cheng, H.; Selloni, A. *Langmuir* **2010**, *26*, 11518.
(32) Li, Y.-F.; Selloni, A. *J. Am. Chem. Soc.* **2013**, *135*, 9195.